Laser cooling of trapped ions

Jürgen Eschner

Institut für Experimentalphysik, Universität Innsbruck, Technikerstrasse 25, A-6020 Innsbruck, Austria

Giovanna Morigi

Abteilung Quantenphysik, University of Ulm, Albert-Einstein-Allee 11, D-89081 Ulm, Germany

Ferdinand Schmidt-Kaler and Rainer Blatt

Institut für Experimentalphysik, Universität Innsbruck, Technikerstrasse 25, A-6020 Innsbruck, Austria

Received November 12, 2002; revised manuscript received December 4, 2002

Trapped and laser-cooled ions are increasingly used for a variety of modern high-precision experiments, for frequency standard applications, and for quantum information processing. Therefore laser cooling of trapped ions is reviewed, the current state of the art is reported, and several new cooling techniques are outlined. The principles of ion trapping and the basic concepts of laser cooling for trapped atoms are introduced. The underlying physical mechanisms are presented, and basic experiments are briefly sketched. Particular attention is paid to recent progress by elucidating several milestone experiments. In addition, a number of special cooling techniques pertaining to trapped ions are reviewed; open questions and future research lines are indicated.

OCIS codes: 140.3320, 300.6520, 270.0270.

1. INTRODUCTION

Laser cooling of atoms and ions has become a routine tool for atomic physics and quantum optics in the past two decades. It provides the basis for many of the modern experiments such as, e.g., the preparation of atomic Bose–Einstein condensates and quantum information processing using atoms and ions for the quantum memory.

Optical cooling of vapors by resonant light, through optical pumping of orientational levels of angular momentum together with successive collisions, was envisioned as early as 1950 by Alfred Kastler.[1] However, it was not before the advent of the tunable laser that optical cooling was seriously reconsidered and proposed as a means to prepare atomic samples for precision spectroscopy. A first generalization of Kastler's ideas was presented in 1974 by Zel'dovich[2] when he proposed to use optical pumping of a two-level system for cooling. Independent proposals for optical cooling of free atoms by use of radiation pressure,[3] and of ions that are bound in an electromagnetic trap,[4] then marked the start of the laser cooling era. Laser cooling was first experimentally observed in 1978 by Neuhauser and coworkers[5] with Ba^+ ions and by Wineland and coworkers with trapped Mg^+ ions.[6] Their seminal papers and the subsequent theoretical work[7,8] spurred more sophisticated and more elaborate investigations of cooling of atoms and ions.

Work with laser-cooled *single* trapped ions was reported first around 1980.[9] It was the starting point of the application of trapped ions to precision spectroscopy[10] and to fundamental quantum optics experiments, such as the observation of quantum jumps.[11–13] Laser cooling of ions in harmonic traps was comprehensively treated by Stenholm[14] and coworkers. Cooling to the quantum mechanical ground state of the trap potential was achieved for the first time by Diedrich *et al.*[15] in the resolved-sideband regime (see below and Ref. 4), using narrowband excitation for the optical pumping.

A renewed investigation of laser cooling of trapped ions started with the development of new laser cooling techniques applied to neutral atoms in standing waves.[16] In particular, treating the cooling of a single harmonically trapped ion in a standing wave[17] led to a new method for the calculation of the cooling dynamics, which proved to be valuable for calculating the production of highly nonclassical states,[18,19] such as Fock states and squeezed states of the ion motion. It was realized that the interaction of a harmonically trapped ion with a light field is virtually equivalent to a Jaynes–Cummings description.[19,20] Thus laser cooling of a trapped ion became the basis for a variety of quantum optical experiments equivalent to cavity quantum electrodynamic experiments.[21,22]

The possibility of manipulating the internal state of a laser-cooled ion with precisely controlled laser pulses led to a whole new branch of quantum optics, now known as quantum state engineering.[23] In particular, quantum information processing with trapped ions was proposed by Cirac and Zoller in 1995.[24] This technique relies entirely on the possibility of achieving ground-state cooling and on the ability to manipulate a quantum state in a well-controlled way. Naturally, this interest stimulated renewed efforts to achieve efficient ground-state cooling, which was obtained, e.g., by use of Raman excitations with Be^+ ions[25] and narrowband optical excitation with Ca^+ ions.[26]

Meanwhile quantum state engineering is being imple-

mented with strings of ions for studies of entanglement[27,28] and for quantum information processing. The required simultaneous cooling of several motional degrees of freedom has been achieved with two ions by Raman sideband cooling[29] and by sympathetic sideband cooling.[30] The necessity to extend ground-state cooling to larger ion strings has led to the invention of conceptually more elaborate, albeit very successful, techniques that use electromagnetically induced transparency (EIT) arising from quantum interference.[31,32]

Laser cooling of trapped ions has deepened our understanding of the mechanical effects of radiation, and it has been instrumental for groundbreaking developments in experimental quantum optics. Today, while it is still an active field of research, it has also become a standard routine in many laboratories, where a variety of cooling procedures are available for precision spectroscopy and quantum optical purposes.

This review paper is outlined as follows: After a brief introduction into the physics of ion traps, the fundamental concepts of laser cooling are outlined in Section 3. The standard cooling procedures, such as Doppler cooling and resolved-sideband cooling, are treated in Section 4, where state of the art and experimental results are summarized. Laser cooling of multilevel systems as well as more elaborate cooling techniques are then reviewed in Section 5, and we conclude with an outline of some open questions and future investigations.

2. ION TRAPS

For the confinement of atomic ions by electromagnetic fields, either a combination of static electric and magnetic fields (Penning trap) or a time-dependent inhomogeneous electric field (Paul trap) is used.[33]

To trap a particle, a restoring force $\mathbf{F} \propto -\mathbf{r}$ is required, where $\mathbf{r}$ is the distance from the origin of the trap. Both types of trap create such a force through a quadrupole potential

$$\Phi = \Phi_0(\alpha x^2 + \beta y^2 + \gamma z^2)/{r_0}^2 \tag{1}$$

where Φ_0 denotes a voltage applied to a quadrupole electrode configuration, r_0 is the characteristic trap size, and the constants α, β, γ determine the shape of the potential. Solving the Laplace equation, we obtain the three-dimensional quadrupole potential described by $\alpha = \beta = -2\gamma$ and a two-dimensional quadrupole potential $\alpha = -\beta$, $\gamma = 0$. The different signs of the factors α, β, γ make it evident that stable confinement cannot be achieved with a static electric potential. Therefore, in three dimensions and with the appropriate sign of the voltage Φ_0 for axial trapping, a magnetic field can be used for radial confinement. This configuration is known as a Penning trap. Without the magnetic field, a time-dependent potential $\Phi_0 = U_{\mathrm{dc}} + V_{\mathrm{ac}}\cos(\Omega_{\mathrm{rf}}t)$ must be used to achieve a stable confinement, which is known as the Paul trap in three dimensions or the Paul mass filter in two dimensions. The latter provides a radial binding force toward the $\hat{z}$ axis and is used, e.g., to guide ion beams and for mass spectrometry.[33,34]

Three-dimensional traps provide a confining force with respect to a single point in space and are therefore used for single-ion experiments or for the confinement of large centrosymmetric ion clouds. Both the Paul and the Penning trap provide a potential that is described by harmonic oscillation in all three dimensions. The axial motion in a Penning trap is governed by the static electric field; the radial motion resulting from the Lorentz forces can be decomposed into a (harmonic) cyclotron and magnetron motion. Thus in a Penning trap the quantum motion of a trapped particle is described by the sum of three harmonic oscillators with frequencies $\nu_{\mathrm{cyc}} \gg \nu_{\mathrm{ax}} \gg \nu_{\mathrm{mag}}$, where, however, the magnetron component contributes with a negative sign, since the electric field forces the ion away from the trap center.

For the Paul trap, stable confinement is achieved by the time dependence of $\Phi(t)$ with appropriately chosen frequency Ω_{rf} and amplitude V_{ac}. With the solution of the resulting (explicitly time-dependent) differential equation, the so-called Mathieu equation, the ion motion in a Paul trap is described by three frequencies of harmonic motion, ν_x, ν_y, ν_z. The amplitude of this secular motion is weakly modulated at the driving frequency Ω_{rf}, the so-called micromotion. The amplitude of that motion increases linearly with the distance of the ion from the trap center. Thus in Paul traps the quantum motion of a single ion located near the trap center is very well approximated by a harmonic oscillation in three dimensions.

The linear variant of the Paul trap is based on the quadrupole mass-filter potential.[35–38] This potential provides confining forces in the two directions perpendicular to the $\hat{z}$ axis, while for axial confinement additional electrodes are attached. The radial confinement is created, as in the three-dimensional Paul trap, by a time-dependent voltage $\Phi_0 = U_{\mathrm{dc}} + V_{\mathrm{ac}}\cos(\Omega_{\mathrm{rf}}t)$ applied to the electrodes. Near the trap axis this creates a potential of the form $\Phi = \Phi_0(x^2 - y^2)/(2{r_0}^2)$, where r_0 denotes the distance from the trap axis to the surface of one of the electrodes. Again, the quantum motion of an ion in the trap is well approximated by harmonic oscillation. Making the radial frequency much higher than the axial one allows trapping of an ion string that is located along the trap axis. The motion of an ion string is described by common harmonic oscillator modes resulting from the equilibrium of the trap's confining potential and the Coulomb repulsion of the neighboring ions. The oscillation frequencies can be readily calculated.[39,40] The lowest frequency ν_z, corresponding to center-of-mass oscillation of the string, equals the single-ion secular frequency, and the highest axial frequency scales approximately as $(2N-1)^{1/2}\nu_z$, where N denotes the number of ions in the string.[39] The two-ion case is discussed in more detail in Subsection 3.D.

In summary, for small amplitudes of the motion, especially for amplitudes that are less than the wavelength of the applied radiation (used for spectroscopy or cooling), the ion motion in these traps can be well approximated by a harmonic oscillation. We mainly concentrate on laser cooling results achieved with three- or two-dimensional Paul traps, in which most quantum optical experiments have been performed. The concepts and methods we present, however, are to a large extent also valid for Penning traps.

3. COOLING OF TRAPPED IONS: CONCEPTS

In this section the fundamental concepts of laser cooling of trapped ions are introduced. The focus is on techniques that allow cooling of the ionic motion to temperatures for which the nonclassical properties of the center-of-mass motion become manifest and that therefore require a quantum mechanical description. We first restrict the discussion to motion along a single motional axis, as this allows for a transparent description without loss of generality. The more general case of cooling in all three spatial dimensions is then introduced. Finally, these concepts are extended to laser cooling of a string of ions.

A. Laser-Cooling of Single Ions

In the absence of other external fields, the center-of-mass motion of a trapped ion with mass M and along the $\hat{z}$ axis is described by the Hamiltonian[41–43]

$$H_{\mathrm{mech}} = \frac{p^2}{2M} + \frac{1}{2}M\nu^2 z^2 = \hbar\nu\left(a^\dagger a + \frac{1}{2}\right). \tag{2}$$

Here ν is the oscillator frequency, p and z are the momentum and the position of the ion, and a and $a^\dagger$ are the annihilation and creation operators of a quantum of vibrational energy $\hbar\nu$, with $z = (\hbar/2M\nu)^{1/2}(a + a^\dagger)$ and $p = i(\hbar M\nu/2)^{1/2}(a^\dagger - a)$. The eigenstates of H_{mech} are the number states $|n\rangle$, $n = 0, 1, 2,...$, at the energies $E_n = \hbar\nu(n + 1/2)$.

The most basic model system for laser cooling is a single trapped ion whose center-of-mass motion is described by Eq. (2) and whose electronic transition, usually an optical dipole transition, is driven by a (quasi-) resonant laser. In the process of photon scattering the total energy of atom and field is conserved, but in the exchange of energy and momentum between atom and radiation, mechanical energy of the atom may be dissipated through spontaneous emission. Under suitably chosen excitation conditions this leads to cooling and to a low steady-state motional energy, as discussed below.

Consider an electronic transition with dipole moment $\mathbf{d}$ and resonance frequency ω_0 driven by monochromatic light at frequency ω_{L} and wave vector $\mathbf{k}$. The laser field is assumed to be classical, and for an ion at position z and at time t it has the form $\boldsymbol{\mathcal{E}}(z, t) = \mathcal{E}_0\boldsymbol{\epsilon}\cos(\omega_{\mathrm{L}}t - k_z z)$, where $\mathcal{E}_0$, $\boldsymbol{\epsilon}$ are amplitude and polarization and $k_z = \mathbf{k}\cdot\hat{z} = |\mathbf{k}|\cos\theta$, with the angle θ between the axis of the motion and the propagation direction of the field. In the rotating-wave approximation and in the reference frame rotating at the laser frequency, the Hamiltonian H of the driven dipole has the form

$$H = H_{\mathrm{mech}} - \hbar\Delta|e\rangle\langle e| + (\hbar\Omega/2) \times [|e\rangle\langle g|\exp(ik_z z) + \mathrm{H.c.}], \tag{3}$$

where $|g\rangle$, $|e\rangle$ denote the ground and excited state of the dipole transition, $\Delta = \omega_{\mathrm{L}} - \omega_0$ is the laser detuning, and $\Omega = \mathbf{d}\cdot\boldsymbol{\epsilon}\mathcal{E}_0/\hbar$ is the Rabi frequency, which is taken to be real with suitable definition of the time $t = 0$. The mechanical effect of light associated with the absorption or emission of a photon is described by the operators $\exp(\pm ik_z z)$: These induce a displacement of the atomic momentum by a quantity $\hbar k_z$ ($-\hbar k_z$) for the absorption (emission) of a laser photon. In the basis of the vibrational states $\{|n\rangle\}$, this is associated with a transition $|n\rangle \rightarrow |n'\rangle$, with probability amplitudes given by the Franck–Condon coefficients $F_{n\rightarrow n'} = \langle n'|\exp(ik_z z)|n\rangle$. Obviously, when $\cos\theta = 0$—i.e., when the laser is perpendicular to the motional axis—there is no exchange of mechanical energy between laser and atom. For $\cos\theta \neq 0$ the average change in mechanical energy that is due to the absorption from (or emission into) the laser mode is the recoil energy $E_{\mathrm{R,laser}} = \hbar\omega_{\mathrm{R}}\cos^2\theta$, where ω_{R} is the recoil frequency defined as

$$\omega_{\mathrm{R}} = \hbar k^2/2M. \tag{4}$$

The full atomic dynamics are described by the master equation for the density matrix ρ of the atom,[44,45]

$$\partial_t\rho = [H, \rho]/i\hbar + \mathcal{L}\rho, \tag{5}$$

where $\mathcal{L}$ is the Liouville operator representing spontaneous decay at the rate Γ on the $|e\rangle \rightarrow |g\rangle$ transition. The spontaneous emission events produce a mechanical effect on the atom as well. On average, because of the spatial symmetry of emission, they do not change the atomic momentum. They affect, however, the ion's mechanical energy, which increases, on average, by the recoil energy $E_{\mathrm{R,spont}} = \hbar\omega_{\mathrm{R}}\alpha$ per event. The factor α describes the average component of the recoil energy on the motional axis, weighted with the dipole pattern of spontaneous emission.[14]

Summarizing, the dynamics of the atomic center-of-mass motion under laser excitation is characterized by three fundamental frequencies: the oscillator frequency ν, the rate of spontaneous emission Γ, and the recoil frequency ω_{R}. Their respective ratios define regimes of laser cooling dynamics. This is well illustrated by discussing their connection to the properties of the dipole absorption spectrum.

The absorption spectrum of the dipole transition is obtained by sweeping the laser detuning Δ across the atomic resonance and looking at the photon scattering rate. For a two-level transition like the one described by Eq. (3), a given state $|g, n\rangle$ is coupled to several excited states $|e, m\rangle$ at Rabi frequencies $\Omega F_{n\rightarrow m}$ and at transition frequencies $\omega_{m-n} = \omega_0 + (m - n)\nu$. Thus the laser can excite a series of resonances spaced by the trap frequency ν. The spectral resolution of these resonances depends on the relation between ν and the linewidth of the transition Γ.[46] For $\Gamma > \nu$ (weak confinement limit) all states $|e, m\rangle$ are excited whose transition frequencies fall inside the resonance curve. On the other hand, for $\Gamma < \nu$ (strong confinement limit) the individual resonances are resolved. This is the so-called sideband spectrum: The resonances appearing at frequencies $\omega_l = \omega_0 + l\nu$ ($l = \pm 1, \pm 2,...$) are the motional sidebands, while the resonance at ω_0 is the carrier. In this limit, the laser can be tuned to a certain (e.g., the lth) sideband, thus selectively driving the transitions between the corresponding vibrational states $|g, n\rangle$ and $|e, n + l\rangle$.

The excitation probability of a sideband is determined by the modulus square of the corresponding Franck–Condon coefficient, whose value depends critically on the relation between ω_{R} and ν. A particularly relevant limit

for laser cooling of trapped ions is the Lamb–Dicke regime $\omega_R \ll \nu$, which is fulfilled when the size of the ground-state wave packet is much smaller than the laser wavelength.[5] In this limit, a hierarchy of transitions between motional states is established that is ordered by the Lamb–Dicke parameter[14] $\eta = (\omega_R/\nu)^{1/2} = (\hbar k^2/2M\nu)^{1/2}$. This hierarchy is applicable to all motional states with vibrational number n such that $(2n + 1)^{1/2}\eta \ll 1$, i.e., whose corresponding wave packet is still well localized over the laser wavelength. The transition at zero order in η is the carrier, involving no change in the vibrational number. The transitions at $\omega_{\pm 1} = \omega_0 \pm \nu$ have a probability of order η^2 and are known as "blue-sideband" $(\omega_0 + \nu)$ and "red-sideband" $(\omega_0 - \nu)$ transitions. For the initial state $|g, n\rangle$, their weight with respect to the carrier is $(n + 1)\eta^2$ and $n\eta^2$, respectively. Transitions involving a larger number of vibrational phonons are of higher order in the Lamb–Dicke parameter and are usually neglected. A typical sideband spectrum in the Lamb–Dicke regime is displayed in Fig. 1. Below, we assume that the Lamb–Dicke regime holds, unless specified otherwise.

These concepts can now be brought together for discussing cooling. Generally, the motion is cooled when transitions to lower energy states are more probable. Thus the laser parameters must be chosen so that red-sideband transitions occur at the higher rate. The optimal values of these parameters depend on the ratio between Γ and ν. To illustrate this, we look more closely at the relevant processes: Below saturation, these are the spontaneous Raman transitions coupling the state $|g, n\rangle$ to $|g, n + 1\rangle$ and $|g, n - 1\rangle$, which happen at rates $R_+ = (n + 1)A_+$ and $R_- = nA_-$, respectively. The rate coefficients $A_\pm$ are given by[14]

$$A_\pm = \frac{\Omega^2}{\Gamma}\eta^2[\cos^2\theta\, W(\Delta \mp \nu) + \alpha W(\Delta)], \qquad (6)$$

with $W(\Delta) = 1/(4\Delta^2/\Gamma^2 + 1)$. Thus the rates $R_\pm$ are the sum of two terms, corresponding to two spontaneous Raman processes scattering the atom into $|g, n \pm 1\rangle$, as illustrated in Fig. 2(a). For instance, the first term of R_+ corresponds to absorption along the blue sideband [with relative probability $(n + 1)\eta^2 \cos^2\theta W(\Delta - \nu)$] followed by spontaneous emission on the carrier (at rate Γ), while the second term describes absorption along the carrier [with relative probability $W(\Delta)$] and spontaneous emission on the sideband [at rate $(n + 1)\eta^2\Gamma$]. These two processes can also be identified with the corresponding components of the fluctuation spectrum of the dipole force and with the diffusion coefficient that is due to spontaneous emission, respectively.[17] It should be pointed out that Eq. (6) describes the rates when the laser is a traveling wave. In the presence of intensity and polarization gradients, additional effects contribute to the scattering process, which may give different weights to the terms on the right-hand side of Eq. (6).[17,47,48]

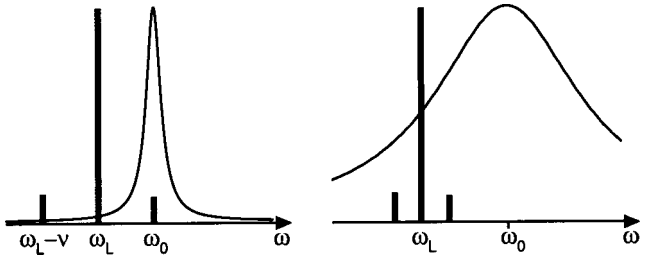

Fig. 1. Illustration of strong confinement (left) and weak confinement (right) in the Lamb–Dicke regime. The Lorentz curve is the atomic resonance of width Γ. The vertical bars display the relative absorption probabilities of the laser and its sidebands, $|F_{n\to m}|^2$ for $m = n, n \pm 1$, at ω_L, $\omega_L \mp \nu$. The laser spectrum is displayed in the reference frame of the ion, with the laser detuned for optimum cooling in both cases, i.e., $\omega_L = \omega_0 - \nu$ and $\omega_L = \omega_0 - \Gamma/2$ for strong and weak confinement, respectively.

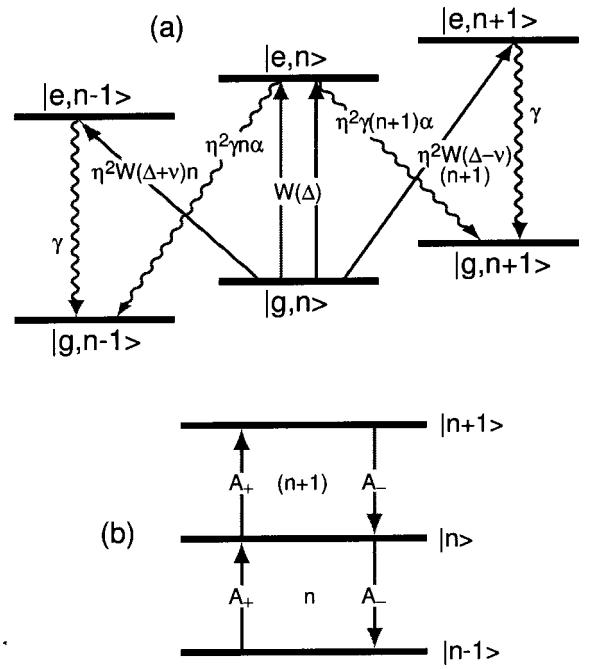

Fig. 2. (a) Cooling $(|n\rangle \to |n - 1\rangle)$ and heating $(|n\rangle \to |n + 1\rangle)$ transitions starting from state $|g, n\rangle$, at lowest order in η. The relative probabilities of the individual processes are indicated for $\cos\theta = 1$. (b) Illustration of the rate coefficients for cooling and heating, after Ref. 14.

The dynamics of the vibrational states are determined by the rates $A_\pm$ and are displayed in Fig. 2(b). The dynamics of the average vibrational number $\langle n\rangle = \Sigma_{n=0}^{\infty} n\langle n|\rho|n\rangle$ are described by[14]

$$\frac{d}{dt}\langle n\rangle = -(A_- - A_+)\langle n\rangle + A_+. \qquad (7)$$

This allows for a steady-state solution when $A_- > A_+$, i.e., when the rate coefficient for red-sideband transitions is larger than that for the blue sideband. This relation is fulfilled for $\Delta < 0$ $(\omega_L < \omega_0)$. In this case Eq. (7) has the solution

$$\langle n\rangle_t = \langle n\rangle_0 \exp[-(A_- - A_+)t] + \bar{n}\{1 - \exp[-(A_- - A_+)t]\}, \qquad (8)$$

where $\langle n\rangle_t$ is the vibrational quantum number at time t and $\bar{n} = A_+/(A_- - A_+)$ is the steady-state value. The form of $\bar{n}$ shows that the lowest values are achieved for large ratios A_-/A_+, while Eqs. (6) and (8) show that the rate at which this value is reached scales with the recoil frequency. From Eq. (6) it can be verified that in the

weak confinement regime ($\Gamma \gg \nu$) the maximum ratio A_-/A_+ is obtained for $\Delta = -\Gamma/2$. This is the case of Doppler cooling, where the steady-state vibrational quantum number for the two-level transition is $\bar{n} \simeq \Gamma/2\nu$.[7,14] This value corresponds to the number of sideband transitions resonantly excited by coupling a motional state $|g, n\rangle$ to $|e\rangle$.

In the strong confinement limit, $\Gamma < \nu$, larger ratios A_-/A_+, and hence lower values of $\bar{n}$, are reached. In this regime of resolved-sideband cooling, cooling is optimized for $\Delta = -\nu$, which corresponds to tuning the laser into resonance with the red sideband, while the carrier and the blue sideband are well off resonance.[7,14] Sideband cooling allows one to obtain very small values of $\bar{n}$. For $\Gamma \ll \nu$, $\bar{n} \simeq (\Gamma/\nu)^2 \ll 1$; i.e., the motional ground state occupation is close to one, and it approaches unity with stronger confinement.

The above considerations show that high cooling efficiency requires a large difference between the red- and the blue-sideband absorption, which can be obtained with a good spectral resolution of the motional sidebands. In the absence of a suitably narrow electronic transition, such resolution may be achieved through the narrow linewidth of multiphoton processes. This idea is the basis of Raman sideband cooling.[49] Here, an effective two-level transition like that in sideband cooling is designed by using a Λ-configuration of atomic levels, where two stable or metastable states $|g_1\rangle$ and $|g_2\rangle$ are coupled by Raman transitions through the common excited state $|e\rangle$.[50] Selective sideband excitation is accomplished by coherent Raman processes that transfer atoms from $|g_1\rangle$ to $|g_2\rangle$, tuned to the red sideband of the two-photon transition. Repumping from $|g_2\rangle$ to $|g_1\rangle$ is achieved with a third laser that induces spontaneous Raman scattering. The linewidth of the process is determined mainly by the linewidth of the spontaneous Raman scattering and can easily be set to yield resolved sidebands. Below, it is shown that this condition may also be achieved by using the narrow lines that are due to quantum interference in the scattering at saturation.[31]

The concepts discussed here can be easily extended to cooling of the motion in all three dimensions. Here, for each axis of the motion (each mode) and in the Lamb–Dicke regime the absorption spectrum is composed of the carrier and the respective blue and red sidebands. These modes can be Doppler cooled or sideband cooled, depending on the ratios between Γ and the frequencies ν_x, ν_y, ν_z of the trap. The angle of $\mathbf{k}$ with the three axes determines how the recoil of a laser photon is divided between the modes, and the recoil energy that is due to a scattered photon is distributed over the modes, depending on the angle of emission. Laser light propagating only along one axis (e.g., $\cos\theta_z = 1$) implies heating in the perpendicular plane. Three-dimensional laser cooling is achieved when laser and trap are configured such that the laser photons have nonvanishing projections on all motional axes.

Throughout this section we have focused on the Lamb–Dicke regime, which is usually encountered in ion trap experiments. Nevertheless, there are situations in which this condition is not fulfilled. It turns out that Doppler cooling is always possible, provided that $\Gamma > \omega_R$.[14] Regarding ground-state cooling outside the Lamb–Dicke regime, there exist some theoretical proposals of how to implement Raman sideband cooling schemes in this situation, and ground-state cooling for relatively large values of η has been predicted.[51,52]

B. Connection to Laser Cooling of Atomic Gases

The way we have represented the cooling mechanism in an ion trap is based on energy eigenstates and accounts for the situation that the motional energy can change only in quanta of the trap energy. This is an adequate description for the Lamb–Dicke regime $\eta \ll 1$, where the recoil energy of a photon is smaller than a motional energy quantum, such that state-changing transitions become suppressed. In contrast, for atomic gases in weakly binding potentials ($\eta > 1$) a description based on momentum eigenstates is more natural, because the recoil momentum of the photon is transferred to an atom in every single absorption and emission event. Still, the final kinetic energy of Doppler cooling turns out to be the same, $\sim\Gamma/2$, for trapped ($\eta \ll 1$) and quasi-free ($\eta > 1$) atoms. Therefore nowadays this type of cooling is referred to as Doppler cooling in both situations. The energy picture, however, had already naturally invoked the concept of sidebands at the initial stage of development, and what is now called Doppler cooling was then consequently denoted sideband cooling.[4–6,9] We stick to the common usage of Doppler cooling for the case $\Gamma > \nu$, but, to avoid confusion, we mostly use the name "resolved-sideband" cooling for the situation of strong confinement ($\Gamma \ll \nu$).

C. Temperature Measurement

The experimental determination of the temperature reached by laser cooling uses the properties of the absorption spectrum, just like cooling itself. The occupation of the vibrational states is measured through absorption or scattering. The most common method is to compare the two absorption probabilities obtained by tuning the laser to the red sideband and to the blue sideband in the strong confinement limit.[15,25,26] Since the state $|g, 0\rangle$ does not contribute to the absorption when the red sideband is excited, the difference between the two probabilities is proportional to the ground-state population. A related method uses comparison of the fluorescence signals on the two sidebands, but there the probe laser must be sufficiently weak that it does not affect the cooling process.[53]

A more precise measurement is obtained by exciting Rabi oscillations.[21,26] Here the blue sideband of the transition between the internal state $|g\rangle$ and a metastable state $|a\rangle$ is driven coherently in the strong confinement regime, and the population of the state $|a\rangle$ is measured as a function of the laser pulse length. This is given by

$$P_a(\tau) = \sum_n \langle g, n|\rho|g, n\rangle \sin^2(\eta\sqrt{n+1}\Omega\tau), \qquad (9)$$

which describes the superposition of Rabi oscillations on each transition $|g, n\rangle \leftrightarrow |a, n+1\rangle$ at the respective Rabi frequency $\eta\sqrt{n+1}\Omega$. Fitting $P_a(\tau)$ to the measured population reconstructs the distribution $P_n = \langle g, n|\rho|g, n\rangle$ at the end of the cooling process.

D. Laser Cooling of Ion Strings

Ion traps can confine several ions. These interact through Coulomb repulsion, and at sufficiently low temperatures they crystallize at the classical equilibrium positions in the total potential given by the trap plus the Coulomb interaction.[54] In linear Paul traps with cylindrical geometry and a steep radial potential,[35] these positions are localized along the trap axis, which is here identified with the $\hat{z}$ axis. The ions form a string,[55,56] and the motion is described by its collective excitations. In the regime usually achieved by Doppler cooling, these excitations are the normal modes of the string, $3N$ eigenmodes for N ions. The axial modes of a string are N harmonic oscillators at frequencies $\nu_\beta\,(\beta = 1 \ldots N)$. In this basis, the displacements q_j of the ions from their classical equilibrium positions $z_j^{(0)}$ are expanded into displacements of all modes with weights determined by both the mode β and the position in the string j.[40] When driven by a laser, the mechanical effect associated with the absorption of a photon by the ion at $z_j^{(0)}$ is described by the operator $\exp(ik_z q_j)$, which is the product of the displacements for each mode. Hence the recoil energy gained by the string after absorption of a photon by one of the ions is distributed over all modes, with weights depending on the position of the ion that undergoes the absorption.

Generally the absorption spectrum of one ion of the string shows a dense distribution of resonances, corresponding to transitions between motional states where the vibrational number of several modes may change simultaneously. In the Lamb–Dicke regime, however, the number of resonances reduces to the carrier resonance and the red and blue sidebands of each mode, i.e., to those transitions where the vibrational number of only one mode may be changed by one phonon. In this limit the modes are individually laser cooled either to the Doppler limit or to the ground state, depending on the linewidth of the excitation process, in the same way as a single ion is cooled.[57–60] Theoretical investigations of laser cooling of Coulomb crystals have confirmed this behavior also outside the Lamb–Dicke regime, where the dynamics of the individual modes cannot be separated.[60] We emphasize that the whole ion string can be cooled by driving a single or a subset of ions, since the displacement of one ion corresponds to a displacement of all modes. This is also the basis of proposals for sympathetic cooling of ion chains,[61,62] where an ion species with favorable transitions for laser cooling is embedded in a chain composed of other species and is used for cooling the motion of the whole chain to the ground state.

4. DOPPLER AND SIDEBAND COOLING: EXPERIMENTS

A. Doppler Cooling

Doppler cooling of trapped ions was first achieved in two experiments in 1978. Using a cloud of $\sim 5 \times 10^4$ Mg^+ ions in a Penning trap, Wineland *et al.* showed that near-resonant laser radiation was able to reduce the temperature to below 40 K.[6] The temperature was measured through currents in the trap electrodes induced by the motion of the ions. With a cloud of ~ 50 Ba^+ ions in a Paul trap, Neuhauser *et al.* demonstrated Doppler cooling by observing a greatly enhanced dwell time of the ions in the trap.[5] The first laser-cooled single ion was prepared later by the same group and in the same apparatus.[9] They estimated a temperature of a few tens of millikelvins from the size of the observed ion image.

Later Doppler cooling was also demonstrated with ions in linear traps,[37,38] in a ring trap,[55,56] and in Penning traps.[63,64] The most prominent feature in this situation is the crystallization of a cloud of ions into a well-ordered linear chain or a three-dimensional Coulomb crystal.[65] This phenomenon was observed through direct imaging of the ions and also through their excitation spectrum.[66,67] A kink appears in the measured dependence of fluorescence rate versus laser detuning when the Doppler-broadened absorption profile of a cloud turns into a narrow (near-natural linewidth) line at the point of crystallization.[68]

Two-component crystals have also been prepared by Doppler cooling one of the two species.[69–71] Such sympathetic cooling works in much the same way as Doppler cooling of a one-component ion cloud. The method has received increased attention recently as it may be useful for ground-state cooling of ions for quantum information processing.[61,62] While one species is continuously laser-excited and the whole string is cooled, the other species is available for coherent quantum manipulations.

B. Resolved-Sideband Cooling to the Vibrational Ground State

This section gives an overview of experiments that have achieved ground-state sideband cooling of single ions and ion crystals. To reach the strong confinement condition, various methods have been established: Either a quadrupole or intercombination transition is excited by a narrowband laser source, or a Raman transition between hyperfine ground states is driven by two laser fields.

1. Resolved-Sideband Cooling on Optical Transitions

The first experiment in which the motional ground state was reached by resolved-sideband cooling was performed on a single trapped $^{198}Hg^+$ ion.[15] The relevant levels of $^{198}Hg^+$ are shown in Fig. 3(a). The $S_{1/2}$ to $P_{1/2}$ transition near 194 nm was used to prepare the ion near the Doppler limit. Then the $S_{1/2}$ to $D_{5/2}$ quadrupole transition near 281 nm was employed to perform sideband cooling. Since the natural lifetime (86 ms) of the $D_{5/2}$ state would put an upper limit to the cooling rate, laser radiation near 398 nm was used to mix the $D_{5/2}$ state with the fast-decaying $P_{3/2}$ state. Thus the width of the $D_{5/2}$ state was increased, and the cooling rate optimized. The ion was stored in a three-dimensional Paul trap with dc control voltages adjusted such that the vibrational frequency was 2.96 MHz in all directions.

For ground-state cooling, the red sideband of the $S_{1/2}$ to $D_{5/2}$ transition was driven for a period of 200–500 ms while the 398-nm radiation was on. The final phonon number $\bar{n}$ after cooling was deduced from the imbalance of the excitation probabilities on the blue and red sidebands of the $S_{1/2}$ to $D_{5/2}$ transition, as explained in Subsection 3.C: The sidebands were excited with a pulse of 15-ms duration, and state-selective fluorescence on the $S_{1/2}$ to $P_{1/2}$ transition revealed whether excitation to $D_{5/2}$

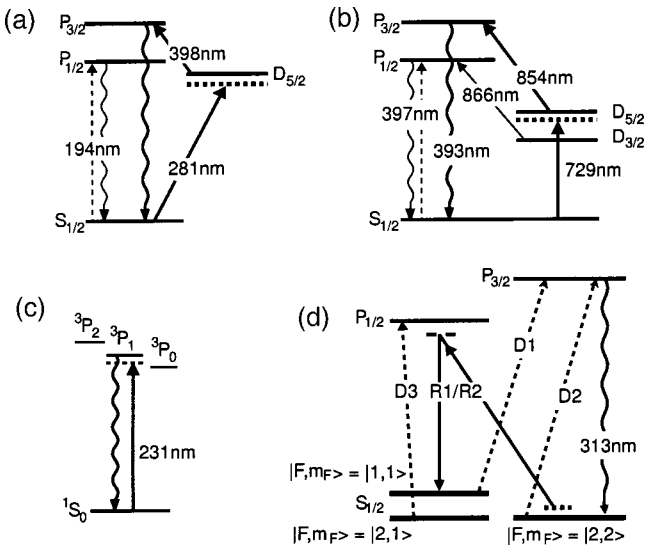

Fig. 3. Levels and transition wavelengths relevant for resolved-sideband cooling in various ion species: (a) With a single $^{198}Hg^+$ ion, Doppler cooling is performed on the transition near 194 nm. For sideband cooling, laser light near 281 and 398 nm is used. The red sideband of the $S_{1/2}$–$D_{5/2}$ transition is indicated with a dashed horizontal line. (b) For Doppler cooling of $^{40}Ca^+$ ions, the dipole transitions near 397 and 866 nm are employed. Resolved-sideband cooling is performed on the quadrupole transition near 729 nm while the dipole transition near 854 nm is used to increase the cooling rate. (c) For resolved-sideband cooling of $^{115}In^+$ ions, the intercombination line near 231 nm is used. (d) Levels relevant for optical cooling of $^9Be^+$ ions. Transitions D1, D2, and D3 are used for Doppler cooling and optical pumping. Raman sideband cooling is performed with laser pulses alternately driving the transitions R1, R2, and D1, D3. All wavelengths are near 313 nm; the hyperfine splitting of both P states is 1.250 GHz.

had happened. The cooling result $\bar{n} = 0.051 \pm 0.012$ corresponds to a 95% ground-state probability.

A single $^{40}Ca^+$ ion was cooled to the ground state by use of the same principle.[26] The level scheme is shown in Fig. 3(b). In this experiment the ion was trapped in a three-dimensional Paul trap with motional frequencies $(\nu_x, \nu_y, \nu_z) = 2\pi(2.16, 2.07, 4.51)$ MHz. Resolved-sideband cooling employed excitation of the narrow $|S_{1/2}, m_J = -1/2\rangle$ to $|D_{5/2}, m_J = -5/2\rangle$ transition near 729 nm, and for efficient cooling the $|D_{5/2}, -5/2\rangle$ state was broadened by a laser near 854 nm, which coupled it to the $|P_{3/2}, -3/2\rangle$ state. Choosing the Rabi frequency at 854 nm optimized either the cooling rate (high Rabi frequency) or the cooling limit (low Rabi frequency). A magnetic field of 400 μT was applied to provide a well-defined quantization axis and Zeeman splitting. The cooling cycle is closed by the decay from $|P_{3/2}, -3/2\rangle$ to $|S_{1/2}, -1/2\rangle$. The cycle can be interrupted, however, since $P_{3/2}$ may decay to $D_{3/2}$, and optical pumping from $D_{3/2}$ to $P_{1/2}$ by laser radiation near 866 nm can bring the system into $|S_{1/2}, +1/2\rangle$. The expected rate for this process is ~1/100 of the cooling rate, estimated from the Clebsch–Gordon coefficients and decay constants. To prevent this leakage of population from the cooling process, short pulses of σ^+ polarized light near 397 nm were used.

After a 2 ms period of precooling on the $S_{1/2}$ to $P_{1/2}$ transition, which brought the ion close to the Doppler limit ($\bar{n}_z \simeq 3$), resolved-sideband cooling was applied. As the cooling time was varied, an exponential decay of the phonon number with decay time 5 ms^{-1} was observed, and a final ground-state population of 99.9% in that vibrational mode (corresponding to $\bar{n}_z = 0.001$) was reached after 6.4 ms of cooling time.

The intercombination line of a trapped $^{115}In^+$ ion was also used for optical cooling.[53] The relevant levels of $^{115}In^+$ are shown in Fig. 3(c). Here, in a three-dimensional Paul trap with typical secular frequencies near 1 MHz, the vibrational sidebands are well resolved when the transition $^1S_0$ to $^3P_1$ with a natural linewidth of $\Gamma/2\pi = 360$ kHz is driven. As was reported in Ref. 53, a mean phonon number below 1 was reached, and both a single ion and a two-ion crystal were prepared in the ground state with 50% probability.

2. Ground-State Cooling of Ion Strings

Ground-state cooling of ion strings works in the same way as the cooling described above. In the resolved-sideband regime, the excitation spectrum exhibits sidebands for each vibrational mode of the string, as explained in Subsection 3.D. The axial modes of a string of $^{40}Ca^+$ ions were observed in Ref. 72. For the case of a two-ion string, the common modes are illustrated in Fig. 4. In the experiment of Ref. 30 only one ion of a two-ion string of $^{40}Ca^+$ was addressed with a tight laser focus. This leads to a situation of sympathetic cooling, as described earlier for two different species: Although the light intensity is concentrated onto one of the ions, all the common vibrational modes are still affected. The ground state of the center-of-mass mode was reached with $\bar{n} \leqslant 0.05$ after 6.4 ms of cooling time.[30]

When all four modes at the frequencies $(\nu_{rad}, \nu_r, \nu_b, \nu_{ax}) = 2\pi(2.0, 1.9, 1.2, 0.7)$ MHz were successively cooled (in this temporal order), mean phonon numbers $(\bar{n}_{rad}, \bar{n}_r, \bar{n}_b, \bar{n}_{ax}) = (2.3, 0.65, 0.47, 0.05)$ were obtained. Because of the sequential cooling technique, the modes that were cooled first were reheated from $\bar{n} \simeq 0.05$ during the cooling of the other modes. The magnitude of reheating can be fully understood from the momentum transfer of the photons scattered in random directions.

3. Raman Sideband Cooling

In the experiments at the National Institute of Standards and Technology, Boulder, hyperfine ground states of $^9Be^+$ ions are employed to encode quantum logic information (qubits), and Raman transitions between these hyperfine

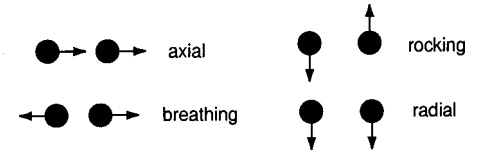

Fig. 4. Illustration of the normal modes of a two-ion string. Left, the common vibration is shown for the axial and breathing modes at frequencies ν_{ax} and $\nu_b = \nu_{ax}\sqrt{3}$, for which the motion is purely along the $\hat{z}$ direction of the trap. Right, radial and rocking modes at frequencies ν_{rad} and $\nu_r = \sqrt{\nu_{rad}^2 - \nu_{ax}^2}$ are depicted.

states are used to implement quantum entanglement operations.[28] To initialize an ion (or ion string) for logic gate operations, Raman sideband cooling is performed. The relevant levels and transitions are defined in Fig. 3(d). In the first cooling experiment[73] a single ion was trapped in a tightly confining Paul trap with vibrational frequencies $(\nu_x, \nu_y, \nu_z) = 2\pi(11.2, 18.2, 29.8)$ MHz. Doppler, cooling on the $S_{1/2}$, $|F = 2, m_F = 2\rangle$ to $P_{3/2}$ transition [beam D2 in Fig. 3(d)] resulted in mean phonon numbers $(\bar{n}_x, \bar{n}_y, \bar{n}_z) = (0.47, 0.30, 0.18)$. Optical pumping into the $S_{1/2}$, $|1, 1\rangle$ and $|2, 1\rangle$ states was prevented with laser light on the transitions labeled D1 and D3. After a 50-μs period of Doppler cooling, the ion was prepared in the $S_{1/2}$, $|2, 2\rangle$ state by switching off beam D2. Then Raman cooling was applied, consisting of two steps: (i) With the relative detuning of the Raman beams set to the first lower sideband, the ion is stimulated from $S_{1/2}$, $|2, 2\rangle$ to $S_{1/2}$, $|1, 1\rangle$, and the mean phonon number is reduced by one. (ii) When light fields D1 and D3 are driven, the ion is recycled to the $S_{1/2}$, $|2, 2\rangle$ state by a spontaneous Raman transition. Five of these cooling cycles were performed in order to reach the vibrational ground state.

To realize cooling in three dimensions, step (i) was cyclically applied with the laser tuned to each of the red sidebands of the x, y, and z vibration. Finally, the mean phonon number was determined from the imbalance of the respective red- and blue-sideband excitation probabilities, yielding $(\bar{n}_x, \bar{n}_y, \bar{n}_z) = (0.033, 0.022, 0.029)$, and thus indicating that the three-dimensional ground state was occupied with 92% probability.[25] The same method was used for simultaneous ground-state cooling of both axial modes of a two-ion string of $^9Be^+$ ions.[29] The result for the axial mode was $\bar{n}_{ax} = 0.11^{+0.17}_{-0.03}$, and for the breathing mode $\bar{n}_b = 0.01^{+0.08}_{-0.01}$.

5. COOLING IN MULTILEVEL SYSTEMS

Comparison of resolved-sideband cooling and Raman sideband cooling shows that these two methods are in fact very similar: Although three (or more) levels are involved in the Raman sideband cooling scheme, they reduce to an effective two-level system, as the upper level can be adiabatically eliminated. The Raman transition takes the role of the narrow optical transition in resolved-sideband cooling, and the repumping corresponds to the spontaneous decay of the upper level (or its quenching via an auxiliary level). Details of the elimination process for different arrangements of levels have been studied in Ref. 50, and the role of branching ratios in the repumping step has been highlighted in Ref. 74.

It is also important to note that in Raman sideband cooling the Raman lasers are tuned into resonance with the $|n\rangle \rightarrow |n - 1\rangle$ transition, just as in sideband cooling. The detuning of both lasers from the intermediate level has to be much larger than the linewidth and can be on either side of the resonance. Slight modifications to the detunings may be required when light shifts caused by the Raman lasers play a role. Such situations have been studied numerically, and optimum parameters have been given for certain cases in Refs. 50 and 75. In Ref. 75 laser cooling in a three-level system driven by two lasers was investigated theoretically in some generality. A numerical study of the same situation, starting from a master equation for the center-of-mass motion, was presented by Reiß *et al.*[76] The calculated results can be interpreted in terms of standard Doppler and Raman sideband cooling processes and intermediate cases. The mathematical procedure allows one to treat all possible light field configurations and can be generalized to more complex level schemes.

A. EIT Cooling

A special case of laser cooling of a three-level system, where light shifts and quantum interference are combined, was recently proposed[31] and experimentally realized.[32] The method uses two lasers coupling two metastable or ground states to the same excited level, one above saturation (the coupling laser), the other below (the cooling laser).[77] The individual transitions may be broad ($\Gamma > \eta$), such that they would normally only allow for Doppler cooling. Both lasers are set above resonance to the same detuning Δ of the order of the linewidth. The intensity of the coupling laser is adjusted such that it creates a light shift of the upper level, which equals the trap frequency. Figure 5 illustrates the arrangement. Provided that the trapped ion is in the Lamb–Dicke regime, this particular combination of detunings and Rabi frequencies has two effects: (i) Carrier ($|n\rangle$ to $|n\rangle$) excitation, which is one source of heating, is suppressed because the two lasers fulfill the EIT (electromagnetically induced transparency[78]) condition for forming a nonabsorbing superposition of the two lower states. (ii) A narrow maximum in the absorption probability of the cooling laser is created that peaks at the frequency of the red-sideband ($|n\rangle \rightarrow |n - 1\rangle$) transition, thus enhancing the cooling. The blue-sideband transition probability can be kept small. Thus, a strong difference between cooling and heating rates is established, and ground-state cooling becomes possible. In fact, this EIT-cooling method is potentially more efficient than resolved-sideband or Raman sideband schemes in the sense that at equal cooling rates the theoretical cooling limit of EIT cooling is lower.[31] Furthermore, the cooling limit does not depend on the orientation of the laser beam with respect to the direction of oscillation because of the suppression of the carrier transitions.

EIT cooling has been experimentally realized with a single trapped Ca^+ ion, utilizing Zeeman substates in the $S_{1/2}$–$P_{1/2}$ state manifold, which is normally used for Doppler cooling.[32] The light fields for coupling and cooling were both derived from the same laser at 397 nm. A ground-state occupation of 90%, corresponding to $\bar{n}_z = 0.1$, was achieved for a single vibrational mode at $\nu_z = 3.32$ MHz, starting from the Doppler cooling limit $\bar{n}_z = 6.5$. It was also shown that simultaneous cooling of two vibrational modes close to the ground state is possible when the light shift is adjusted to a value between the two vibrational frequencies.

The practical advantages of EIT cooling over other ground-state cooling methods are its experimental simplicity and its easy combination with Doppler cooling. Its applicability to various systems, including neutral atoms in dipole traps and strings of ions for quantum infor-

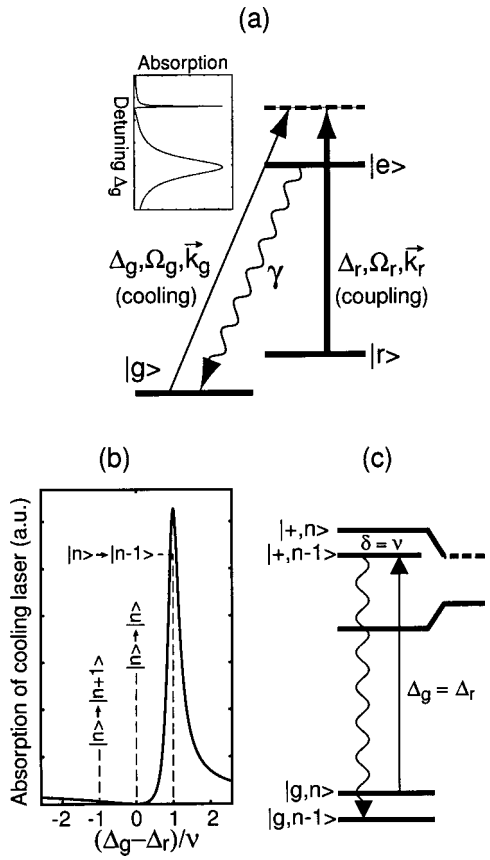

Fig. 5. (a) Levels and transitions of the EIT-cooling scheme. The coupling laser drives $|r\rangle \rightarrow |e\rangle$, the cooling laser $|g\rangle \rightarrow |e\rangle$. The inset shows schematically the absorption rate on $|g\rangle \rightarrow |e\rangle$ when the atom is strongly excited above resonance on $|r\rangle \rightarrow |e\rangle$.[76] (b) Absorption of cooling laser around $\Delta_g = \Delta_r$ (solid curve); dashed lines mark the probabilities of carrier ($|n\rangle \rightarrow |n\rangle$) and sideband ($|n\rangle \rightarrow |n \pm 1\rangle$) transitions for the case $\Delta_g = \Delta_r$. (c) Dressed-state picture: the cooling laser excites resonantly transitions from $|g, n\rangle$ to the narrow dressed state denoted $|+, n-1\rangle$, which preferentially decays into $|g, n-1\rangle$. δ is the light shift (ac Stark shift) created by the coupling laser.

mation processing, has been considered and tested in simulations.[79,80] Further experiments will have to confirm this potential.

B. Other Cooling Methods

The laser cooling methods described so far, Doppler, (Raman) sideband, and to some extent EIT cooling, are the standard tools presently used in ion trap experiments. A few less conventional methods have also been proposed, and some of them have been experimentally demonstrated.

1. Sisyphus Cooling

Sisyphus cooling was first developed for quasi-free neutral atoms and can be achieved with multilevel atoms in light fields with polarization gradients[81] or intensity gradients.[82] In several theoretical studies it has also been considered for trapped ions. Wineland *et al.*[47] treat the case of a three-level atom that is confined to the Lamb–Dicke regime by a trapping potential and that interacts, on one transition, with an off-resonant standing-wave light field. The ion must be positioned at the point of maximum gradient in the standing wave. They find that, as in the case of free atoms, the cooling limit is given by the well depth of the standing-wave light potential and that sub-Doppler cooling to an energy near the ground state of the trapping potential can be achieved. Using a trapped Mg^+ ion as an example, $\bar{n} = 1.23$ is calculated for a situation where the Doppler limit is $\bar{n} \approx 10$. A similar result is found in Refs. 83 and 48 for polarization gradient cooling of a trapped ion in the Lamb–Dicke limit. In the specific case of a $j = 1/2 \rightarrow j = 3/2$ transition in a lin⊥lin molasses light field, a cooling limit of $\bar{n} \approx 1$ is calculated.

The case of polarization gradient cooling looks easier to implement experimentally, because the requirement of a well-defined position of the ion relative to the light field is lifted.[48] Yet neither of the Sisyphus cooling techniques has so far been put into practice, i.e., applied to an ion trapped in the Lamb–Dicke regime. Polarization gradient cooling of a single ion was studied experimentally only under conditions where the trapping potential along the cooled direction was shallow,[84] similar to typical conditions with neutral atoms. The final temperature of the cooling process was in agreement with the free-atom results. The same setup was later used to study anomalous diffusion processes in an optical lattice.[85,86]

2. Cooling by State Selection

A rather different technique, able to prepare a single ion in the motional ground state in a more probabilistic way, was proposed in Ref. 87. It uses sideband excitation to a long-lived upper state, as in sideband cooling, but the cooling cycle is not completed by spontaneous emission or quenching of the upper level. Instead, state-selective fluorescence is utilized to probe the internal state of the ion after the sideband excitation pulse, as shown in Fig. 6(a). If fluorescence is observed, the ion is in the lower state of the cooling transition, whereas no fluorescence indicates that it resides in the upper state. If now, after initial excitation to the upper level, a long series of alternating blue-sideband excitation and probe pulses is recorded, where all measurements show *no* fluorescence, then the ion will eventually be found close to the motional ground state. For a motional state of a given purity there is a corresponding number of consecutive no-fluorescence results that have to be detected to obtain that state. If that number is not reached in one run, i.e., fluorescence appears too early, another sequence has to be started. Owing to its probabilistic character, the method was initially called stochastic cooling.[87]

It may first appear contradictory that without photon scattering the ion loses motional energy, but what really happens is that an initially cold ion is selected. As illustrated in Fig. 6(b), the absence of fluorescence reveals information about the motional state: Since the sideband Rabi frequency for $|n\rangle \leftrightarrow |n-1\rangle$ transitions scales as $\sqrt{n}$, deexcitation from the upper state by a blue-sideband pulse is less likely for a colder ion. Therefore every consecutive no-fluorescence result makes it more probable that the ion is in a low-lying motional state. Although the method is no standard cooling technique where the motional energy is dissipated, a cooling rate—or inverse

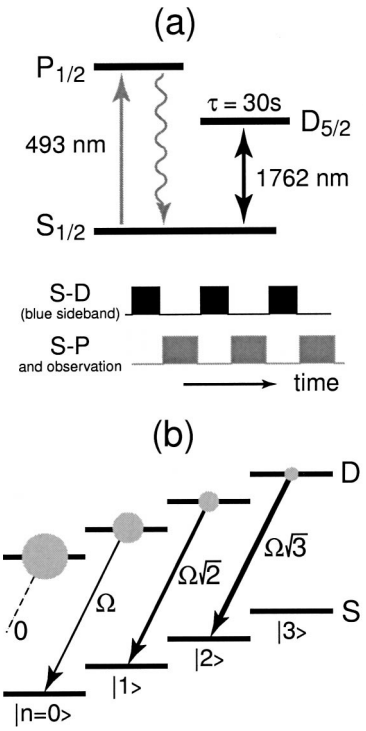

Fig. 6. Schematic of cooling by detection of no fluorescence: (a) Simplified level scheme showing the slow cooling transition $S-D$ and the fast transition for state-selective fluorescence $S-P$. The Ba^+ ion is taken as an example. Blue-sideband excitation on $S-D$ is alternated with probing on $S-P$. (b) Starting in some distribution over the motional states in D (gray circles), the higher-lying states are more likely to be deexcited (arrows). The $|D, n+1\rangle \leftrightarrow |S, n\rangle$ Rabi frequencies are indicated. If the ion is in $|D, n=0\rangle$, it will remain dark.

cooling time—can be defined as in standard schemes: For any motionally excited initial state, there is a certain measurement time, including unsuccessful runs, after which the desired state (or probability distribution) is obtained.[87]

A signature of the cooling process just described was observed in an experiment with a single Ba^+ ion.[88] The transition at 1762 nm between the $S_{1/2}$ ground state and the long-lived $D_{5/2}$ state ($\tau \approx 30$ s) was excited with sideband pulses, while alternating resonant excitation on the $S_{1/2} \rightarrow P_{1/2}$ dipole transition yielded state-selective fluorescence. It was observed that, starting from $D_{5/2}$, the probability for deexcitation indeed decreases with an increasing number of preceding consecutive no-fluorescence results, thus confirming that a longer no-fluorescence series yields a colder ion.

Similar techniques, where state-dependent information is employed to select the cold part of an ensemble, have later been suggested and demonstrated for neutral atoms.[89,90] They have also been called "informational cooling"[90] and were linked to the idea of Maxwell's demon.[89]

3. Other Dark-State Cooling Techniques

All ground-state cooling mechanisms for trapped ions rely on the decoupling of the lowest energy state from the exciting light field(s); i.e., the final state of the cooling process is a dark state. A corresponding method for free atoms is velocity-selective coherent population trapping (VSCPT),[91] where a dark superposition of momentum states is created. It was theoretically shown that such dark superposition states, involving two vibrational modes, also exist in ion traps and that they may be created in a laser cooling process.[92] The method, however, has not been tested experimentally.

6. SUMMARY AND OUTLOOK

Laser cooling has become a routine tool in many laboratories and especially in atomic and molecular physics, e.g., in the investigation of cold quantum gases and trapping of atoms with optical fields. Applications for precision spectroscopy, for time and frequency standards, and for quantum information processing are fundamentally relying on the ability to prepare quantum states at will by using laser cooling techniques.

Ions confined in traps were the very first sample with which laser cooling was demonstrated, and a single laser-cooled ion today still represents one of the best understood objects for fundamental investigations of the interaction between matter and radiation. Moreover, laser cooling of a trapped atom makes it possible to invoke very powerful and fast optical cooling mechanisms as, e.g., the resolved-sideband cooling technique outlined above. Experiments with single trapped ions spurred the development of similar methods with trapped atoms in optical potentials and still provide the ideal testing ground for many new ideas. Two particular advantages of single laser cooled ions in traps are that they can be confined to very small spatial regions (below one optical wavelength) and that they can be prepared and controlled at will for experiment times exceeding days. Measuring and controlling the final quantum state of a trapped ion is then possible with resolved-sideband spectroscopy. For this purpose new methods for the detection of the sidebands and thus the characterization of the cooling have been advantageously developed with single ions,[93] and they are still under investigation.

With samples of trapped ions crystallization has been investigated: Plasma physics at the extremely low temperature limit has become possible, a regime which was not accessible without efficient laser cooling. Thus, long-ranging correlations arising from the Coulomb interaction can be studied, which make the crystal a large-scale quantum matter with properties that are not entirely explored yet.

Aside from being the testing ground and the ideal tool for the demonstration of fundamental concepts and ideas, laser-cooled ions have become the workhorse for many modern precision measurements, and they will be the basis for future technologies. New atomic clocks based on measuring an optical transition of a single trapped ion indicate that accuracy figures of 10^{-18} are within reach.[94] This in turn will lead to a substantially increased precision of all experiments relying on time keeping and frequency measurements.

The underlying features of trapped ion experiments, such as the ability to precisely localize a single atom, to prepare it in a pure quantum state, and to detect its state

by the electron shelving technique, make trapped ions the ideal tool for storing and manipulating quantum information. This potential has led to renewed efforts in developing laser cooling methods, particularly for trapped ion strings. Information storage and manipulation in trapped atoms and ions also requires increasing control of the pertaining quantum states. The concepts and experimental methods involved in such quantum state engineering have been developed out of laser cooling procedures, and these two fields are still profiting from their mutual stimulation. Thus, it can be expected that laser cooling of trapped atomic and ionic structures, which are to be used as quantum registers, will receive ongoing interest.

In conclusion, laser cooling of trapped ions provides a key building block for a broad range of cutting-edge experiments, and it will become a basic feature for many future investigations and applications. Of particular interest would be to achieve laser cooling of naturally trapped atoms such as, e.g., atomic impurities in crystals or in larger molecules. Using the currently available cooling techniques would then allow one to do laser cooling of molecules or even bulk material. These possibilities are being realized, and the first experiments are being carried out.[95–97] Thus it may be expected that laser cooling of trapped atoms and ions will also become a key technology in molecular and solid-state physics.

ACKNOWLEDGMENTS

This work is supported by the European Commission (Quest network, HPRN-CT-2000-00121, Qubits network, IST-1999-13021), by the Austrian Fonds zur Förderung der wissenschaftlichen Forschung (SFB15), and by the Institut für Quanteninformation GmbH.

J. Eschner may be reached at Juergen.Eschner @uibk.ac.at.

REFERENCES AND NOTES

1. A. Kastler, "Quelques suggestions concernant la production optique et la détection optique d'une inégalité de population des niveaux de quantification spatiale des atomes," J. Phys. **11**, 255–265 (1950).
2. Ya. B. Zel'dovich, "Cooling with the aid of high-frequency energy," JETP Lett. **19**, 74–75 (1974).
3. T. W. Hänsch and A. L. Schawlow, "Cooling of gases by laser radiation," Opt. Commun. **13**, 68–69 (1975).
4. D. Wineland and H. Dehmelt, "Proposed $10^{14}\delta\nu/\nu$ laser fluorescence spectroscopy on Tl^+ mono-ion oscillator III (side band cooling)," Bull. Am. Phys. Soc. **20**, 637 (1975).
5. W. Neuhauser, M. Hohenstatt, P. Toschek, and H. Dehmelt, "Optical-sideband cooling of visible atom cloud confined in parabolic well," Phys. Rev. Lett. **41**, 233–236 (1978).
6. D. J. Wineland, R. E. Drullinger, and F. L. Walls, "Radiation-pressure cooling of bound resonant absorbers," Phys. Rev. Lett. **40**, 1639–1642 (1978).
7. D. J. Wineland and W. M. Itano, "Laser cooling of atoms," Phys. Rev. A **20**, 1521–1540 (1979).
8. W. M. Itano and D. J. Wineland, "Laser cooling of ions stored in harmonic and Penning traps," Phys. Rev. A **25**, 35–54 (1982).
9. W. Neuhauser, M. Hohenstatt, P. E. Toschek, and H. Dehmelt, "Localized visible Ba^+ mono-ion oscillator," Phys. Rev. A **22**, 1137–1140 (1980).
10. D. J. Wineland, W. M. Itano, and R. S. van Dyck, "High resolution spectroscopy of stored ions," Adv. At. Mol. Phys. **19**, 135–186 (1983).
11. W. Nagourney, J. Sandberg, and H. Dehmelt, "Shelved optical electron amplifier: observation of quantum jumps," Phys. Rev. Lett. **56**, 2797–2799 (1986).
12. Th. Sauter, W. Neuhauser, R. Blatt, and P. E. Toschek, "Observation of quantum jumps," Phys. Rev. Lett. **57**, 1696–1698 (1986).
13. J. C. Bergquist, R. Hulet, W. M. Itano, and D. J. Wineland, "Observation of quantum jumps in a single atom," Phys. Rev. Lett. **57**, 1699–1702 (1986).
14. S. Stenholm, "Semiclassical theory of laser cooling," Rev. Mod. Phys. **58**, 699–739 (1986), and references therein.
15. F. Diedrich, J. C. Bergquist, W. M. Itano, and D. J. Wineland, "Laser cooling to the zero-point energy of motion," Phys. Rev. Lett. **62**, 403–406 (1989).
16. Special Issue of J. Opt. Soc. Am. B **6**, (1989).
17. J. I. Cirac, R. Blatt, P. Zoller, and W. D. Phillips, "Laser cooling of trapped ions in a standing wave," Phys. Rev. A **46**, 2668–2681 (1992).
18. J. I. Cirac, A. S. Parkins, R. Blatt, and P. Zoller, "Dark squeezed states of the motion of a trapped ion," Phys. Rev. Lett. **70**, 556–559 (1993).
19. J. I. Cirac, R. Blatt, A. S. Parkins, and P. Zoller, "Preparation of Fock states by observation of quantum jumps in an ion trap," Phys. Rev. Lett. **70**, 762–765 (1993).
20. C. A. Blockley, D. F. Walls, and H. Risken, "Quantum collapses and revivals in a quantized trap," Europhys. Lett. **17**, 509–514 (1992).
21. D. M. Meekhof, C. Monroe, B. E. King, W. M. Itano, and D. J. Wineland, "Generation of nonclassical motional states of a trapped atom," Phys. Rev. Lett. **76**, 1796–1799 (1996).
22. M. Brune, F. Schmidt-Kaler, A. Maali, J. Dreyer, E. Hagley, J. M. Raimond, and S. Haroche, "Quantum Rabi oscillation: a direct test of field quantization in a cavity," Phys. Rev. Lett. **76**, 1800–1803 (1996).
23. J. I. Cirac, A. S. Parkins, R. Blatt, and P. Zoller, "Nonclassical states of motion in ion traps," Adv. Atom., Mol., Opt. Phys. **37**, 237–296 (1996).
24. J. I. Cirac and P. Zoller, "Quantum computations with cold trapped ions," Phys. Rev. Lett. **74**, 4091–4094 (1995).
25. C. Monroe, D. M. Meekhof, B. E. King, S. R. Jefferts, W. M. Itano, and D. J. Wineland, "Resolved-sideband Raman cooling of a bound atom to the 3D zero-point energy," Phys. Rev. Lett. **75**, 4011–4014 (1995).
26. Ch. Roos, Th. Zeiger, H. Rohde, H. C. Nägerl, J. Eschner, D. Leibfried, F. Schmidt-Kaler, and R. Blatt, "Quantum state engineering on an optical transition and decoherence in a Paul trap," Phys. Rev. Lett. **83**, 4713–4716 (1999).
27. Q. A. Turchette, C. S. Wood, B. E. King, C. J. Myatt, D. Leibfried, W. M. Itano, C. Monroe, and D. J. Wineland, "Deterministic entanglement of two trapped ions," Phys. Rev. Lett. **81**, 3631–3634 (1998).
28. C. A. Sackett, D. Kielpinski, B. E. King, C. Langer, V. Meyer, C. J. Myatt, M. Rowe, Q. A. Turchette, W. M. Itano, D. J. Wineland, and C. Monroe, "Experimental entanglement of four particles," Nature **404**, 256–259 (2000).
29. B. E. King, C. S. Wood, C. J. Myatt, Q. A. Turchette, D. Leibfried, W. M. Itano, C. Monroe, and D. J. Wineland, "Cooling the collective motion of trapped ions to initialize a quantum register," Phys. Rev. Lett. **81**, 1525–1528 (1998).
30. H. Rohde, S. T. Gulde, C. F. Roos, P. A. Barton, D. Leibfried, J. Eschner, F. Schmidt-Kaler, and R. Blatt, "Sympathetic ground state cooling and coherent manipulation with two-ion-crystals," J. Opt. B **3**, S34–S41 (2001).
31. G. Morigi, J. Eschner, and C. H. Keitel, "Ground state laser cooling using electromagnetically induced transparency," Phys. Rev. Lett. **85**, 4458–4461 (2000).
32. C. F. Roos, D. Leibfried, A. Mundt, F. Schmidt-Kaler, J. Eschner, and R. Blatt, "Experimental demonstration of ground state laser cooling with electromagnetically induced transparency," Phys. Rev. Lett. **85**, 5547–5550 (2000).
33. P. K. Gosh, *Ion Traps* (Clarendon, Oxford, UK, 1995).

34. P. Kienle, "Sunshine by cooling," Naturwissenschaften **88**, 313–321 (2001), and references therein.
35. J. Prestage, G. J. Dick, and L. Maleki, "New ion trap for frequency standard applications," J. Appl. Phys. **66**, 1013–1017 (1989).
36. G. R. Janik and L. Maleki, "Simple analytic potentials for linear ion traps," J. Appl. Phys. **67**, 6050–6055 (1990).
37. M. G. Raizen, J. M. Gilligan, J. C. Bergquist, W. M. Itano, and D. J. Wineland, "Ionic crystals in a linear Paul trap," Phys. Rev. A **45**, 6493–6501 (1992).
38. M. G. Raizen, J. M. Gilligan, J. C. Bergquist, W. M. Itano, and D. J. Wineland, "Linear trap for high accuracy spectroscopy of stored ions," J. Mod. Opt. **39**, 233–242 (1992).
39. A. Steane, "The ion trap quantum information processor," Appl. Phys. B **64**, 623–642 (1997).
40. D. V. F. James, "Quantum dynamics of cold trapped ions, with application to quantum computation," Appl. Phys. B **66**, 181–190 (1998).
41. In the absence of applied fields the trapped ion may still couple to the environment: Heating and decoherence of quantum states of the motion has been observed,[42] the origin of which is partly still unclear. Apparently this effect is critically determined by the trap characteristics, and the rate can be much slower than the rate of laser cooling.[43] Furthermore, the charge of the ion couples to blackbody radiation. This process is also negligible on the time scales considered here. In the discussion, we ignore these effects.
42. Q. A. Turchette, D. Kielpinski, B. E. King, D. Leibfried, D. M. Meekhof, C. J. Myatt, M. A. Rowe, C. A. Sackett, C. S. Wood, W. M. Itano, C. Monroe, and D. J. Wineland, "Heating of trapped ions from the quantum ground state," Phys. Rev. A **61**, 063418 (2000).
43. D. J. Wineland, C. Monroe, W. M. Itano, D. Leibfried, B. E. King, and D. M. Meekhof, "Experimental issues in coherent quantum-state manipulation of trapped atomic ions," J. Res. Natl. Inst. Stand. Technol. **103**, 259–328 (1998).
44. S. Stenholm, "Redistribution of molecular velocities by optical processes," Appl. Phys. **15**, 287–296 (1978).
45. C. Cohen-Tannoudji, J. Dupont-Roc, and G. Grynberg, *Atom–Photon Interactions* (Wiley, New York, 1992).
46. When the natural linewidth is comparable with or smaller than the laser linewidth, the rate Γ has to be replaced by the spectroscopic linewidth obtained experimentally.
47. D. J. Wineland, J. Dalibard, and C. Cohen-Tannoudji, "Sisyphus cooling of a bound atom," J. Opt. Soc. Am. B **9**, 32–42 (1992).
48. J. I. Cirac, R. Blatt, A. S. Parkins, and P. Zoller, "Laser cooling of trapped ions with polarization gradients," Phys. Rev. A **48**, 1434–1445 (1993).
49. D. J. Heinzen and D. J. Wineland, "Quantum-limited cooling and detection of radio-frequency oscillations by laser-cooled ions," Phys. Rev. A **42**, 2977–2994 (1990).
50. I. Marzoli, J. I. Cirac, R. Blatt, and P. Zoller, "Laser cooling of trapped three-level ions: designing two-level systems for sideband cooling," Phys. Rev. A **49**, 2771–2779 (1994).
51. G. Morigi, J. I. Cirac, M. Lewenstein, and P. Zoller, "Ground-state laser cooling beyond the Lamb–Dicke limit," Europhys. Lett. **39**, 13–18 (1997).
52. L. Santos and M. Lewenstein, "Dynamical cooling of trapped gases: one-atom problem," Phys. Rev. A **59**, 613–619 (1999).
53. E. Peik, J. Abel, Th. Becker, J. von Zanthier, and H. Walther, "Sideband cooling of ions in radio-frequency traps," Phys. Rev. A **60**, 439–449 (1999).
54. In experiments the distance among the ions is usually of several wavelengths, and the only relevant interaction is the Coulomb repulsion. For distances of the order of the wavelength, the dipole–dipole interaction must be taken into account. Its effect in connection with laser cooling has been investigated in A. W. Vogt, J. I. Cirac, and P. Zoller, "Collective laser cooling of two trapped ions," Phys. Rev. A **53**, 950–968 (1995).
55. I. Waki, S. Kassner, G. Birkl, and H. Walther, "Observation of ordered structures of laser-cooled ions in a quadrupole storage ring," Phys. Rev. Lett. **68**, 2007–2010 (1992).
56. G. Birkl, S. Kassner, and H. Walther, "Multiple-shell structures of laser-cooled $^{24}Mg^{+}$ ions in a quadrupole storage ring," Nature **357**, 310–313 (1992).
57. J. Javanainen, "Light-pressure cooling of a crystal," Phys. Rev. Lett. **56**, 1798–1801 (1986).
58. J. Javanainen, "Laser cooling of trapped-ion clusters," J. Opt. Soc. Am. B **5**, 73–81 (1988).
59. G. Morigi, J. Eschner, J. I. Cirac, and P. Zoller, "Laser cooling of two trapped ions: sideband cooling beyond the Lamb–Dicke limit," Phys. Rev. A **59**, 3797–3808 (1999).
60. G. Morigi and J. Eschner, "Doppler cooling of a Coulomb crystal," Phys. Rev. A **64**, 063407 (2001).
61. D. Kielpinski, B. E. King, C. J. Myatt, C. A. Sackett, Q. A. Turchette, W. M. Itano, C. Monroe, and D. J. Wineland, "Sympathetic cooling of trapped ions for quantum logic," Phys. Rev. A **61**, 032310 (2000).
62. G. Morigi and H. Walther, "Two-species Coulomb chains for quantum information," Eur. Phys. J. D **13**, 261–269 (2001).
63. S. L. Gilbert, J. J. Bollinger, and D. J. Wineland, "Shell-structure phase of magnetically confined strong coupled plasmas," Phys. Rev. Lett. **60**, 2022–2025 (1988)
64. J. N. Tan, J. J. Bollinger, B. Jelenkovic, and D. J. Wineland, "Long-range order in laser-cooled, atomic-ion Wigner crystals observed by Bragg scattering," Phys. Rev. Lett. **75**, 4198–4201 (1995).
65. A discussion of crystallization in these mesoscopic structures is beyond the scope of this work. The interested reader can find a review in D. H. Dubin and T. M. O'Neil, "Trapped nonneutral plasmas, liquids, and crystals (the thermal equilibrium state)," Rev. Mod. Phys. **71**, 87–172 (1999).
66. F. Diedrich, E. Peik, J. M. Chen, W. Quint, and H. Walther, "Observation of a phase transition of stored laser-cooled ions," Phys. Rev. Lett. **59**, 2931–2934 (1987).
67. D. J. Wineland, J. C. Bergquist, W. M. Itano, J. J. Bollinger, and C. H. Manney, "Atomic-ion Coulomb clusters in an ion trap," Phys. Rev. Lett. **59**, 2935–2938 (1987).
68. R. Blümel, J. M. Chen, E. Peik, W. Quint, W. Schleich, Y. R. Shen, and H. Walther, "Phase transition of stored laser-cooled ions," Nature **334**, 309–313 (1988).
69. D. S. Hall and G. Gabrielse, "Electron cooling of protons in a nested Penning trap," Phys. Rev. Lett. **77**, 1962–1965 (1996).
70. W. Alt, M. Block, P. Seibert, and G. Werth, "Spatial separation of atomic states in a laser-cooled ion crystal," Phys. Rev. A **58**, R23–R25 (1998).
71. P. Bowe, L. Hornekær, C. Brodersen, M. Drewsen, J. S. Hangst, and J. P. Schiffer, "Sympathetic crystallization of trapped ions," Phys. Rev. Lett. **82**, 2071–2074 (1999).
72. H. C. Nägerl, D. Leibfried, F. Schmidt-Kaler, J. Eschner, and R. Blatt, "Coherent excitation of normal modes in a string of Ca^{+} ions," Opt. Express **3**, 89–96 (1998).
73. C. Monroe, D. M. Meekhof, B. E. King, S. R. Jefferts, W. M. Itano, and D. J. Wineland, "Resolved-sideband Raman cooling of a bound atom to the 3D zero-point energy," Phys. Rev. Lett. **75**, 4011–4014 (1995).
74. G. Morigi, H. Baldauf, W. Lange, and H. Walther, "Raman sideband cooling in the presence of multiple decay channels," Opt. Commun. **187**, 171–177 (2001).
75. M. Lindberg and J. Javanainen, "Temperature of laser-cooled trapped three-level ion," J. Opt. Soc. Am. B **3**, 1008–1017 (1986).
76. D. Reiß, A. Lindner, and R. Blatt, "Cooling of trapped multilevel ions: a numerical analysis," Phys. Rev. A **54**, 5133–5140 (1996).
77. While we give the original explanation here, a more recent study shows that EIT cooling works without restrictions on the intensities see the two lasers, as long as the Lamb–Dicke limit applies; see G. Morigi, "Cooling atomic motion with quantum interference," Phys. Rev. A (to be published); preprint available at http://arXiv.org/abs/quant-ph/0211043.
78. E. Arimondo, "Coherent population trapping in laser spectroscopy," in *Progress in Optics XXXV*, pp. 257–354, E. Wolf, ed. (North Holland, Amsterdam, 1996).

79. S. E. Harris, "Electromagnetically induced transparency," Phys. Today **50**(7), 36–42 (1997), and references therein.
80. F. Schmidt-Kaler, J. Eschner, G. Morigi, C. F. Roos, D. Leibfried, A. Mundt, and R. Blatt, "Laser cooling with electromagnetically induced transparency: application to trapped samples of ions or neutral atoms," Appl. Phys. B **73**, 807–814 (2001).
81. J. Dalibard and C. Cohen-Tannoudji, "Laser cooling below the Doppler limit by polarization gradients: simple theoretical models," J. Opt. Soc. Am. B **6**, 2023–2045 (1989).
82. J. Dalibard and C. Cohen-Tannoudji, "Dressed-atom approach to atomic motion in laser light: the dipole force revisited," J. Opt. Soc. Am. B **2**, 1707–1720 (1985).
83. S. M. Yoo and J. Javanainen, "Polarization gradient cooling of a trapped ion," Phys. Rev. A **48**, R30–R33 (1993).
84. G. Birkl, J. A. Yeazell, R. Rückerl, and H. Walther, "Polarization gradient cooling of trapped ions," Europhys. Lett. **27**, 197–202 (1994).
85. H. Katori, S. Schlipf, and H. Walther, "Anomalous dynamics of a single ion in an optical lattice," Phys. Rev. Lett. **79**, 2221–2224 (1997).
86. S. Schlipf, H. Katori, L. Perotti, and H. Walther, "Diffusion of a single ion in a one-dimensional optical lattice," Opt. Express **3**, 97–103 (1998).
87. J. Eschner, B. Appasamy, and P. E. Toschek, "Stochastic cooling of a trapped ion by null detection of its fluorescence," Phys. Rev. Lett. **74**, 2435–2438 (1995).
88. B. Appasamy, Y. Stalgies, and P. E. Toschek, "Measurement-induced vibrational dynamics of a trapped ion," Phys. Rev. Lett. **80**, 2805–2808 (1998).
89. T. Binnewies, U. Sterr, J. Helmcke, and F. Riehle, "Cooling by Maxwell's demon: preparation of single-velocity atoms for matter-wave interferometry," Phys. Rev. A **62**, 011601 (2000).
90. V. I. Balykin and V. S. Letokhov, "Informational cooling of neutral atoms," Phys. Rev. A **64**, 063410 (2001).
91. A. Aspect, E. Arimondo, R. Kaiser, N. Vansteenkiste, and C. Cohen-Tannoudji, "Laser cooling below the one-photon recoil energy by velocity-selective coherent population trapping," Phys. Rev. Lett. **61**, 826–829 (1988).
92. R. Dum, P. Marte, T. Pellizzari, and P. Zoller, "Laser cooling to a single quantum state in a trap," Phys. Rev. Lett. **73**, 2829–2832 (1994).
93. Ch. Raab, J. Eschner, J. Bolle, H. Oberst, F. Schmidt-Kaler, and R. Blatt, "Motional sidebands and direct measurement of the cooling rate in the resonance fluorescence of a single trapped ion," Phys. Rev. Lett. **85**, 538–541 (2000).
94. R. J. Rafac, B. C. Young, J. A. Beall, W. M. Itano, D. J. Wineland, and J. C. Bergquist, "Sub-dekahertz ultraviolet spectroscopy of $^{199}Hg^{+}$," Phys. Rev. Lett. **85**, 2462–2465 (2000).
95. R. I. Epstein, M. I. Buchwald, B. C. Edwards, T. R. Gosnell, and C. E. Mungan, "Observation of laser-induced fluorescent cooling of a solid," Nature **377**, 500–503 (1995).
96. J. L. Clark and G. Rumbles, "Laser cooling in the condensed phase by frequency up-conversion," Phys. Rev. Lett. **76**, 2037–2040 (1996).
97. C. W. Hoyt, M. Sheik-Bahae, R. I. Epstein, B. C. Edwards, and J. E. Anderson, "Observation of anti-Stokes fluorescence cooling in thulium-doped glass," Phys. Rev. Lett. **85**, 3600–3603 (2000).